

ON THE MEASUREMENT OF THE SOUND ABSORPTION OF NON-FLAT BARRIERS

M Garai & A Cocchi

DIENCA, University of Bologna, Viale Risorgimento 2, 40136 Bologna, Italy

1. INTRODUCTION

The importance of the sound absorption of noise barriers to control the sound reflected by the barrier surfaces is widely acknowledged, but the methods currently used to evaluate this absorption are not appropriate to the actual conditions of installation and usage of the barriers or are not yet fully developed. An effective test method to be used in situ is therefore highly desirable. This paper presents some recent experiences made by the authors with the MLS method of measuring the sound absorption in situ [1], in the frame of the European project *Adrienne*.

2. THE MEASUREMENT TECHNIQUE

The selected method was the echo-impulse one, which allows to obtain the sound reflection factor, and hence the sound absorption coefficient, by comparing the acoustic signals impinging on and reflecting from the sample under test. The method was implemented using a repeated MLS as source signal [1]. It is worth noting that this signal permits to get valid results in presence of a high background noise, even with a $S/N=0$ dB, as experienced in the preliminary phase of *Adrienne*. The following devices were used (Fig. 1):

- Sound source: AL/105. It is a closed cabinet, bass-reflex, two-way diffusor with the possibility to switch on or off the woofer alone, the tweeter alone or both of them. Amplifier included in the cabinet.
- Microphone: Brüel & Kjær type 4190 (1/2" inch).
- Microphone pre-amplifier: Brüel & Kjær type 2669.
- Microphone power supply: Brüel & Kjær type 2807.
- A2D-160 board: it contains the MLS generator, the programmable 8-pole anti-aliasing filter and the A/D converter (having an effective resolution of 16 bits).

- Toshiba T6600C portable computer, containing the A2D-160 board.
- Software's: MLSSA software supplied with the A2D-160 board [2], for the acquisition of the impulse responses; ALFA, a special-purpose software under development at DIENCA, for the signal processing.

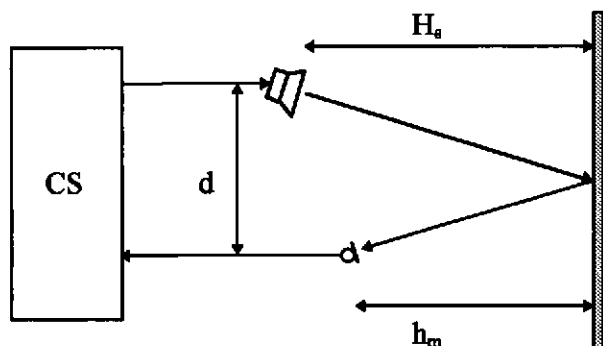


Figure 1. Sketch of the measurement set-up for the MLS echo-impulse method at oblique incidence. The loudspeaker cabinet includes also the amplifier. CS is the "control system" comprising: the microphone power supply, the MLS generator, the anti-aliasing filter; the A/D converter and the clock. The last four components are built on the A2D-160 board mounted into the PC.

The signal received at the measuring microphone is:

$$p_m(t) = p_i(t) + K_r p_i(t) * r_p(t - \tau) + \sum_j K_{r,j} p_i(t) * r_{p,j}(t - \tau_j) + p_n(t) \quad (1)$$

where: $p_i(t)$ is the direct contribution from the sound source, $r_p(t - \tau)$ is the reflection factor of the surface under test, the j -terms are interpreted as the unwanted reflections from the environment, $p_n(t)$ is the extraneous background noise, $*$ is the symbol of convolution, K_r is the geometrical spreading factor accounting for the path length difference between the direct and reflected signals and τ is the delay time resulting from the same path length difference [1].

In the time domain, the impulse response of the material under test is:

$$p_r(t) = K_r p_i(t) * r_p(t - \tau) \quad (2)$$

This one and the direct wave $p_i(t)$ can be extracted from the microphone signal, eq. (1), using a suitable windowing function, provided that the amplitude of $p_i(t)$ decays to an insignificant value with respect to $p_r(t)$

within the time delay τ . From a Fourier transformation of eq. (2) the sound power reflection factor $|R_p(f)|^2$ can then be obtained:

$$|R_p(f)|^2 = \frac{1}{K_r^2} \left| \frac{P_r(f)}{P_i(f)} \right|^2 \quad (3)$$

from which the sound absorption coefficient can be easily computed. The direct and the reflected pulses in eq. (1) should be well separable each other and from parasitic reflections. This is feasible if the pulses are as sharp as possible. Thus, the impulse sharpening technique suggested by Wilms and Heinz [3] was adopted. For doing this, it is necessary to have the impulse response of the measurement chain, $p_{mc}(t)$, which is in practice dominated by the sound source impulse response, $p_d(t)$:

$$p_{mc}(t) \approx p_d(t) = K_d p_i(t) * \delta(t - \tau_d) \quad (4)$$

where the appropriate geometrical factor and delay time are shown. Two FFT give the spectra of the microphone signal, eq. (1), and of the impulse response of the measurement chain, eq. (4); the first is divided by the second and the result is anti-transformed in the time domain. In this way, the impulse response of the measurement chain is deconvolved from the single impulses contained in the microphone signal, sharpening the impulses contained in the eq. (1) by the length of the diffusor impulse response. The authors implemented this technique taking the direct wave as the impulse response of the measurement chain: this eliminates the need to have an independent measurement of $p_{mc}(t)$ and allows an automatic procedure to be performed.

3. RESULTS

Among the various materials to be tested during the preliminary phase of the *Adrienne* project, one is of particular interest here: a medium absorbing non-flat mix of mineralised wood and cement (Beton Bois) in tiles of 0,50x0,50 m, 130 mm thick (Fig. 2). A sample of 2,50x2,50 m (25 tiles) was tested at normal incidence (0°) and oblique incidence (30°) and with three orientations of the tiles:

- orientation a: tiles laid down with all the grooves equally oriented;
- orientation b: tiles laid down with the grooves randomly oriented;
- orientation c: tiles laid down with all the grooves equally oriented, but in the direction orthogonal to the orientation a.

The results are expressed as values of the sound absorption coefficient as a function of frequency, in 1/3 octave bands from 100 Hz to 5000 Hz (Figg. 3, 4, 5, 6). The measurements for the orientations a and c gave similar results.

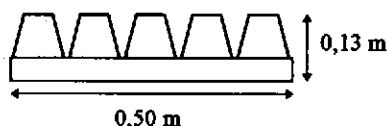


Figure 2. Sketch of a Beton Bois tile (side view).

4. CONCLUSION

The results for a non-flat material show a sound absorption greater than expected, especially at low frequency. At oblique incidence the apparent sound absorption is even increased in the entire frequency range of measurement. The most important reason for this is the role of the diffusion, which is not easily separable from the "true" absorption. Measurements done on other flat samples, such as rockwool battens, didn't give such a strong diffusion effect. This is of particular importance for the designers of noise control solutions: barriers made from hard and non-flat materials are often claimed to have a low sound reflection factor, but actually this is due to diffusion, i.e. to the scattering of sound in non-specular directions, rather than to an effective absorption mechanism. In the typical configuration of two parallel barriers erected alongside a road, this scattered noise will persist to propagate between the two barriers, hitting the drivers and being finally re-directed against some fixed receiver, making the noise control goals partly fail. Therefore, it should be desirable to test anti-noise barriers under a directive sound field with different angles of incidence rather than under a diffuse sound field (like in ISO 354:1985 [4]) and to put in evidence the possible presence of a strong diffusion effect when presenting the sound absorption values.

5. ACKNOWLEDGEMENT

The results presented here are part of the preliminary phase of the European project *Adrienne* ("Test method for the acoustic performance of road traffic noise reducing devices"), funded by the European Commission (contract MAT1-CT94049). The main partners of the research are: Acoustical Technologies (B), Fraunhofer Institut für Bauphysik (D), ENTPE-LASH (F) and DIENCA (I).

6. REFERENCES

- [1] M.Garai, Appl. Acoust., 39, 119 (1993).
- [2] D.D.Rife "MLSSA Reference manual vr.7.0", DRA Labs, USA (1991).
- [3] U.Wilms, R.Heinz, Acustica, 75, 28 (1991).
- [4] ISO 354:1985 "Acoustics - Measurement of sound absorption in a reverberation room", Geneva, Switzerland.

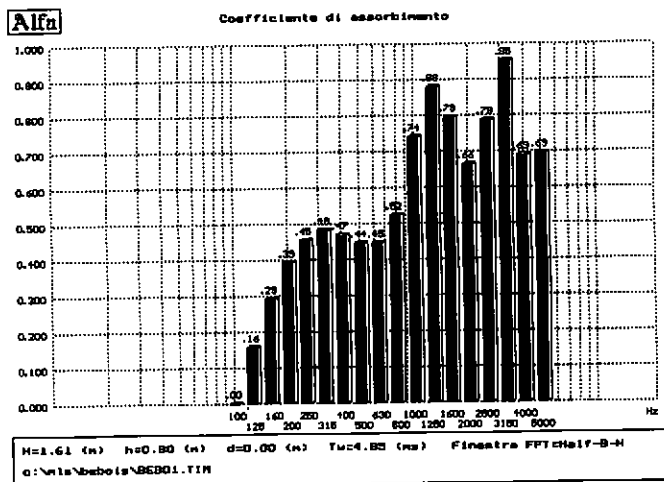


Figure 3. Sound absorption coefficient. Normal incidence, orientation a.
 $H_s=1,61$ m; $h_m=0,80$ m; $T_w=4,49$ ms.

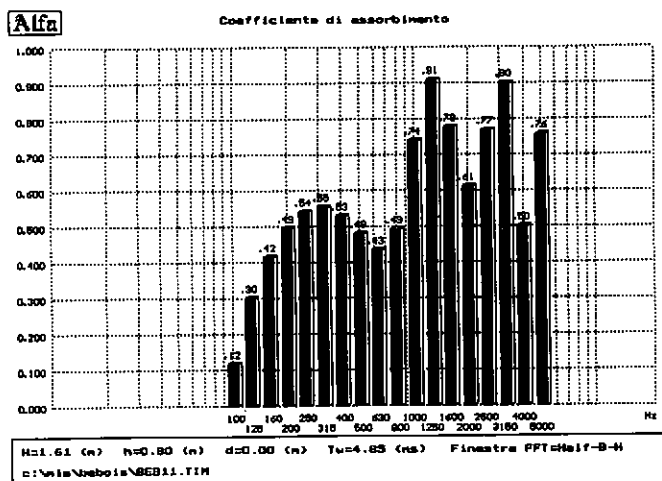


Figure 4. Sound absorption coefficient. Normal incidence, orientation b.
 $H_s=1,61$ m; $h_m=0,80$ m; $T_w=4,49$ ms.

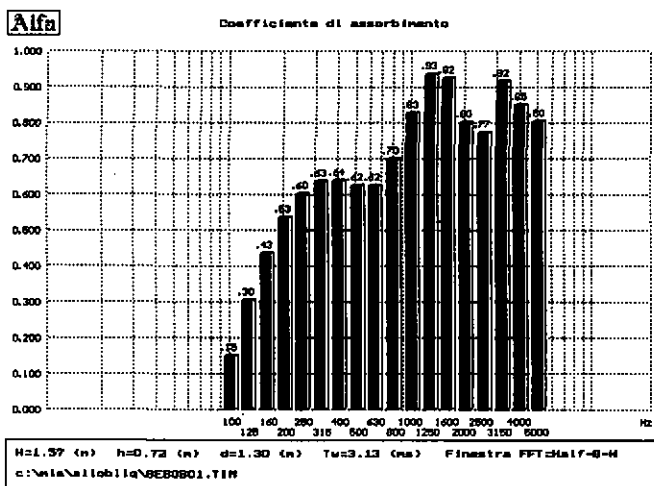


Figure 5. Sound absorption coefficient. 30° oblique incidence, orientation a. $H_s=1,57$ m; $h_m=0,72$ m; $d=1,30$ m; $T_w=3,13$ ms.

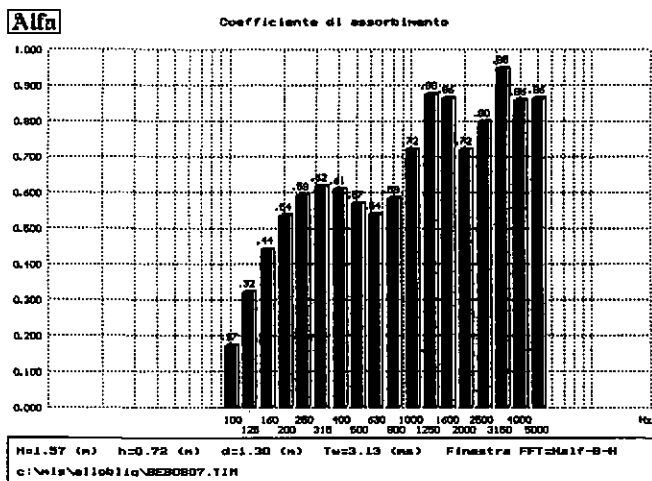


Figure 6. Sound absorption coefficient. 30° oblique incidence, orientation b. $H_s=1,57$ m; $h_m=0,72$ m; $d=1,30$ m; $T_w=3,13$ ms.